JAST
Journal of Aerospace Science and Technology

Pages: 47-60/ Vol.15/ No.2 / Summer- Fall 2022

Journal of Aerospace Science and Technology

www:jast.ias.ir

Scientific-Research Article

Reducing inertial navigation error using Tightly coupled integrated INS/GPS Structure

Amir Moghtadaei Rad [1]
Electerical Engineering, Hashtgerd Branch, Islamic Azad, University,Alborz, Iran

ABSTRACT

Inertial navigation amplifies the noise of the input sensors over time due to the presence of an integrator in the output path to determine the position and attitude of the object. This system has high bandwidth and good short-term accuracy. On the other hand, GPS navigation has low bandwidth, low noise processing power, and long-term accuracy. However, it can only determine the position and does not give us information about the object's attitude. Most papers have presented integrated algorithms related to GPS/INS tightly coupled navigation and have provided relatively acceptable results. Nevertheless, the main problem in this integration model is when there is an intentional or stochastical signal interference for GPS, which is not far from the mind in military applications. Therefore, navigation faces a problem. This article provides a solution with a tightly coupled integrated algorithm for high accuracy in integrated navigation.

***Keywords**: Integrated navigation, Tightly coupled, GPS, INS, Kalman filter*

Introduction

In general, navigation is the science of determining the position and attitude of an object on land, air, or sea. Navigation is usually divided into two general forms, namely blind navigation and navigation using an external signal. Inertial navigation, which uses three accelerometer sensors and three gyroscope sensors to determine the position and attitude of the object, is placed under the first category, and navigation using GPS is placed under the second category. If the information is received from 3 GPS, the position is determined in two dimensions, i.e., the longitude and latitude of the object. Moreover, when it is received from 4 GPS, height is added to the position components of the object, and the three-dimensional position of the object is determined.

Inertial navigation has fast dynamics, high bandwidth, and low sampling time. However, its input error increases and causes deviations in position, velocity, and output attitude. These problems are due to noise sources on its sensors, including accelerometer bias, gyroscope drift, and two integrators in the output path. Therefore, this type of navigation does not have good long-term accuracy despite good short-term accuracy.

Hence, special inertial sensors with high accuracy and low noise are required for accurate navigation applications, which are very expensive. Also, their manufacturing and sales monopoly is in possession of several superior countries. Therefore, it is not easily accessible, especially in military applications.

1 Assistant Professor **Email:** Amir.moghtadaei@hiau.ac.ir

DOI: 10.22034/jast.2022.306926.1099
Submit: 27.09.2021 / Accepted: 16.10.2022
Print ISSN:1735-2134 Online ISSN: 2345-3648

GPS, on the other hand, has low bandwidth, high sampling time, and much more accurate positioning than inertial navigation in the long run. However, it can only determine the position and not the attitude. It also has limitations in speed and height in determining the position. For example, it is impossible to determine the position at speeds higher than 515 meters per second or altitudes higher than 18 kilometers due to restrictions imposed by manufacturing countries.
In addition, the probability of signal interference in GPS signals in military wars is very high. Therefore, their information may be associated with interference [1-4].
Consequently, the scientists combined the navigation of inertial and GPS to use a variety of integrated algorithms to take advantage of both navigation systems and cover each other's disadvantages. Much work has been done over the years in the field of integrated inertial navigation and GPS. Although they can estimate the position, velocity, and attitude, accelerometer errors, and gyroscope errors, and improve their navigation accuracy, the design of integrated tightly coupled algorithms has been neglected.
This paper estimates all states of flying objects with high accuracy by a tightly coupled integration algorithm. Compared to other methods, this method is related to acceptable estimation during the outage of GPS signal in a short or long time. They have not achieved the results with this precision among the gps outage signal.

Sources of error in inertial navigation

Sources of error in accelerometers:

1- Fixed bias:

This error is a constant value equal to $\boldsymbol{B_a}$, the amount of deviation of the accelerometer output from its ideal value, which is independent of time.

$$\iint_0^t \boldsymbol{B_a d\tau} = \boldsymbol{B_a}\frac{\boldsymbol{t^2}}{\boldsymbol{2}}$$

2- White noise:

This error adds a Random process noise with zero mean and $\boldsymbol{\sigma^2}$ variance to the value measured by the accelerometer.

Noise at the output will be a 2nd degree random walk with a mean of zero and the following standard deviation:

$$\boldsymbol{\sigma_s(t) = \sigma \times t^{3/2} \times \sqrt{\frac{\delta t}{3}}}$$

This noise is usually the result of mechanical or thermal disturbances in accelerometers that appear as follows.

3- Calibration:
Errors known as non-alignment errors, conversion factor errors, and nonlinearity errors are generally included in this category. These errors are referred to as calibration errors that are proportional to the input.

4- Bias instability:
These errors indicate the amount of bias fluctuations over a period of time, which means how much the accelerometer bias changes over a period of time, such as in an hour or a second. These errors are also modeled as random walks (VRW1).

Sources of error in gyroscopes:

1- Fixed bias:
This error is a constant value equal to $\boldsymbol{B_g}$, the amount of deviation of the gyroscope output from its ideal value, which is independent of time.

$$\iint_0^t \boldsymbol{B_g d\tau} = \boldsymbol{B_g}\frac{\boldsymbol{t^2}}{\boldsymbol{2}}$$

2- White noise:
This error adds a Random process noise with zero mean and $\boldsymbol{\sigma^2}$ variance to the value measured by the accelerometer.
Noise at the output will be a first-degree random walk with a mean of zero and the following standard deviation:

$$\boldsymbol{\sigma_\theta(t) = \sigma \times \sqrt{\delta t \times t}}$$

This noise is usually the result of mechanical or thermal disturbances in gyroscopes that appear as follows.

Calibration:

Errors known as non-alignment errors, conversion factor errors, and nonlinearity errors are generally included in this category. These errors are referred

1 Velocity Random Walk

to as calibration errors that are proportional to the input.

Bias instability:

These errors indicate the amount of bias fluctuations over a period of time, which means how much the Accelerometer bias change over a period of time, such as in an hour or a second. These errors are also modeled as random walks (ARW**2**).

From the perspective of random processes, the sources of error in inertial navigation are divided into two general categories:

1- deterministic **3** error sources: Parts 1 and 3 of the previous section fall into this category and can be removed by calibration.

1- stochastic **4** error sources: Sections 2 and 4 of the previous section fall into this category and should be randomly modeled and removed by the Kalman filter or any optimal estimator. These sources of error are each divided into 2 categories:

- **Low frequency noises**

(Turn on bias + in run bias (bias drift))

- **High frequency noises**

(Velocity random walk**5** and angular random walk**6** noises)

They are known as random walkers, and it is better to remove them from the system before entering the Kalman filter during the noise decomposition and denoising process.

An example of the types of noise mentioned above for different types of inertial navigation systems is as follows:

Table 2-1: Specifications of different types of noise in different types of inertial navigation systems[8,9]

Parameter	IMU Grade		
	Navigation	Tactical	MEMS
Accelerometers			
In Run Bias (mg)	0.025	1	2.5
Turn On Bias (mg)	-	-	30
Scale Factor (PPM)	100	300	10000
VRW (g/√Hz)	-	2.16e-06	370e-06
Gyros			
In Run Bias (°/h)	0.0022	1	<1040
Turn On Bias (°/h)	-	-	5400
Scale Factor (PPM)	5	150	10000
ARW (°/h/√Hz)	6.92	7.5	226.8
Approx. Cost	>$90000	>$20000	<$2000

Therefore, assuming the elimination of the fixed part of the errors through calibration, the general model of the output error of the accelerometer and gyroscope will be as follows:

$$\boldsymbol{\delta f_b = \delta b + w_f}$$

Where δb is the low frequency noise of accelerometer and δb is the high frequency noise of accelerometer.

Therefore, the Gauss Markov Grade 1 model for low frequency noise of the accelerometer is as follows:

$$\delta \dot{b} = -\alpha \delta b + w_b \qquad w_b = \sqrt{2\alpha\sigma^2}w(t) \qquad \alpha = \frac{1}{\tau_{ba}}$$

Where, σ is the noise of the Gauss-Markov process and τ_{ba} is the correlation time.

$$\delta w_b = \delta d + w_w$$

Where, δd is the low frequency noise of gyroscope and w_w is the high frequency noise of gyroscope.

Therefore, the Gauss Markov Grade 1 model for low frequency noise of the gyroscope is as follows:

$$\delta \dot{d} = -\beta \delta d + w_d \qquad w_d = \sqrt{2\beta\sigma^2}w(t) \qquad \beta = \frac{1}{\tau_{bg}}$$

Where σ is the noise of the Gauss-Markov process and τ_{bg} is the correlation time.

The parameters of the Gauss-Markov model are obtained as follows: after the static test of the inertial measuring unit (IMU) for a certain period of time, for example, 8 hours, the data obtained are first separated by high and low-frequency noise analysis methods and high-frequency noises are separated from the low-frequency noises.

Then their autocorrelation function (ACS or ACF) is calculated. The autocorrelation function of Gauss-Markov random processes is exponential ($R_{bb}(\tau) = \sigma_b^2 e^{-\beta_1 \tau}$). Therefore, by adapting the Gauss-Markov function of degree 1 to the autocorrelation curve obtained from the data, parameters and then the Gauss-Markov model The bottom is determined [5-10].

2 Angular Random Walk
3 Deterministic
4 Stochastic
5 VRW
6 ARW

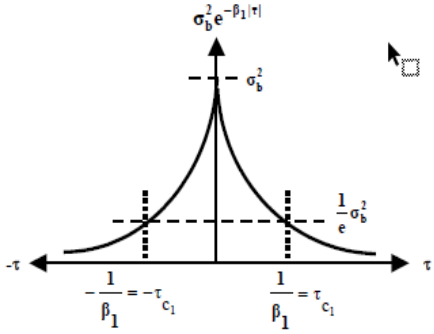

Figure 2-1: Gauss-Markov function curve of degree 1[10]

Modeling the state error in inertial navigation (previous estimate)

According to the above, the following models for low frequency noise of accelerometer and gyroscope as well as 15-state model of system error were obtained:

Grade 1 Gauss Markov model for accelerometers:

$$\begin{bmatrix}\dot{b}_1\\ \dot{b}_2\\ \dot{b}_3\end{bmatrix}=\begin{bmatrix}\frac{-1}{\tau_{bax}} & 0 & 0\\ 0 & \frac{-1}{\tau_{bay}} & 0\\ 0 & 0 & \frac{-1}{\tau_{baz}}\end{bmatrix}\begin{bmatrix}b_1\\ b_2\\ b_3\end{bmatrix}+\begin{bmatrix}\sqrt{2\alpha_x\sigma^2}\\ \sqrt{2\alpha_y\sigma^2}\\ \sqrt{2\alpha_z\sigma^2}\end{bmatrix}\mathrm{w(t)}$$

Grade 1 Gauss Markov model for gyroscopes:

$$\begin{bmatrix}\dot{d}_1\\ \dot{d}_2\\ \dot{d}_3\end{bmatrix}=\begin{bmatrix}\frac{-1}{\tau_{bgx}} & 0 & 0\\ 0 & \frac{-1}{\tau_{bgy}} & 0\\ 0 & 0 & \frac{-1}{\tau_{bgz}}\end{bmatrix}\begin{bmatrix}d_1\\ d_2\\ d_3\end{bmatrix}+\begin{bmatrix}\sqrt{2\beta_x\sigma^2}\\ \sqrt{2\beta_y\sigma^2}\\ \sqrt{2\beta_z\sigma^2}\end{bmatrix}\mathrm{w(t)}$$

15-State model for inertial navigation error:

Position error model:

$$\delta\dot{\underline{r}}^n = F_{rr}.\delta\underline{r}^n + F_{rv}.\delta\underline{v}^n$$

$$F_{rr}=\begin{bmatrix}0 & 0 & \frac{v_N}{(M+h)^2}\\ \frac{v_E\sin\varphi}{(N+h)\cos^2\varphi} & 0 & \frac{v_E}{(N+h)^2\cos\varphi}\\ 0 & 0 & 0\end{bmatrix}$$

$$F_{rv}=\begin{bmatrix}\frac{1}{M+h} & 0 & 0\\ 0 & \frac{1}{(N+h)\cos\varphi} & 0\\ 0 & 0 & 1\end{bmatrix}$$

Velocity error model:

$$\delta\dot{\underline{v}}^n = F_{vr}\delta\underline{r}^n + F_{vv}\delta\underline{v}^n + (\underline{f}^n_{in}\times)\underline{\varepsilon}^n + C_b^n\delta b$$

$$F_{vr}=\begin{bmatrix}2v_E\omega_e\cos\varphi & \frac{{v_E}^2}{(N+h)\cos^2\varphi} & 0 & \frac{v_Nv_D}{(M+h)^2}+\frac{{v_E}^2\tan\varphi}{(N+h)^2}\\ 2\omega_e(v_D\sin\varphi+v_N\cos\varphi)+\frac{v_Ev_N}{(N+h)\cos^2\varphi} & 0 & \frac{v_Ev_D}{(N+h)^2} & \frac{v_Nv_E\tan\varphi}{(N+h)^2}\\ 2v_E\omega_e\sin\varphi & 0 & \frac{{v_E}^2}{(N+h)^2}+\frac{{v_N}^2}{(M+h)^2} & \frac{2\gamma}{R+h}\end{bmatrix}$$

$$F_{vv}=\begin{bmatrix}\frac{v_D}{M+h} & 2\omega_e\sin\varphi & \frac{2v_E\tan\varphi}{N+h} & \frac{v_N}{M+h}\\ 2\omega_e\sin\varphi+\frac{v_E\tan\varphi}{N+h} & \frac{v_D}{N+h}+\frac{v_N\tan\varphi}{N+h} & 2\omega_e\cos\varphi+\frac{v_E}{N+h}\\ 2\frac{v_N}{M+h} & 2\omega_e\cos\varphi & 2\frac{v_E}{N+h} & 0\end{bmatrix}$$

Attitude error model:

$$\dot{\underline{E}}^n = \underbrace{F_{er}\delta\underline{r}^n + F_{ev}\delta\underline{v}^n}_{\delta\underline{\omega}^n_{in}} \quad (\underline{\omega}^n_{in}\times)\underline{\varepsilon}^n \quad C_b^n\delta d$$

$$F_{er}=\begin{bmatrix}\omega_e\cos\varphi & 0 & \frac{v_E}{(N+h)^2}\\ 0 & 0 & \frac{v_N}{(M+h)^2}\\ \omega_e\cos\varphi & \frac{v_E}{(N+h)\cos^2\varphi} & 0 & \frac{v_E\tan\varphi}{(N+h)^2}\end{bmatrix}$$

$$F_{ev}=\begin{bmatrix}0 & \frac{1}{N+h} & 0\\ \frac{1}{M+h} & 0 & 0\\ 0 & \frac{\tan\varphi}{N+h} & 0\end{bmatrix}$$

$$\omega_{in}^{n} = \begin{bmatrix} 2\omega_e \cos\varphi + \frac{v_E}{N+h} \\ \frac{v_N}{M+h} \\ 2\omega_e \sin\varphi \quad \frac{v_E \tan\varphi}{N+h} \end{bmatrix}$$

Equations will also be true for accelerometers and gyroscopes [11-15].
We will reach the following model by aggregating the above relations:

$$\dot{X}(t) = FX(t) + Gw(t)$$

$$w(t) = N(0.Q)$$

$$\begin{bmatrix} \dot{\boldsymbol{r}} \\ \dot{\boldsymbol{v}} \\ \dot{\boldsymbol{\varepsilon}} \\ \dot{\boldsymbol{\delta b}} \\ \dot{\boldsymbol{\delta d}} \end{bmatrix} = \begin{bmatrix} \boldsymbol{F_{rr}} & \boldsymbol{F_{rv}} & \boldsymbol{0} & \boldsymbol{0} & \boldsymbol{0} \\ \boldsymbol{F_{vr}} & \boldsymbol{F_{vv}} & \boldsymbol{f_{in}^{n}\times} & \boldsymbol{C_b^n} & \boldsymbol{0} \\ \boldsymbol{F_{er}} & \boldsymbol{F_{ev}} & \boldsymbol{-\omega_{in}^{n}\times} & \boldsymbol{0} & \boldsymbol{-C_b^n} \\ \boldsymbol{0} & \boldsymbol{0} & \boldsymbol{0} & \frac{\boldsymbol{-1}}{\boldsymbol{\tau_{ba}}} & \boldsymbol{0} \\ \boldsymbol{0} & \boldsymbol{0} & \boldsymbol{0} & \boldsymbol{0} & \frac{\boldsymbol{-1}}{\boldsymbol{\tau_{bg}}} \end{bmatrix} \begin{bmatrix} \boldsymbol{r} \\ \boldsymbol{v} \\ \boldsymbol{\varepsilon} \\ \boldsymbol{\delta b} \\ \boldsymbol{\delta d} \end{bmatrix} + \begin{bmatrix} \boldsymbol{0} & \boldsymbol{0} & \boldsymbol{0} & \boldsymbol{0} \\ \boldsymbol{C_b^n} & \boldsymbol{0} & \boldsymbol{0} & \boldsymbol{0} \\ \boldsymbol{0} & \boldsymbol{C_b^n} & \boldsymbol{0} & \boldsymbol{0} \\ \boldsymbol{0} & \boldsymbol{0} & \boldsymbol{I} & \boldsymbol{0} \\ \boldsymbol{0} & \boldsymbol{0} & \boldsymbol{0} & \boldsymbol{I} \end{bmatrix} \begin{bmatrix} \boldsymbol{w_f} \\ \boldsymbol{w_w} \\ \boldsymbol{w_b} \\ \boldsymbol{w_d} \end{bmatrix}$$

To obtain the variance of the noises to use them in the Kalman filter,
it is sufficient to obtain their autocorrelation function at zero due to their white characteristic, which is equal to the power signal.
The power signal is equal to the sum of the squares of the mean and the variance of the noise. As the mean of the white noise is zero, the power will be the same as the variance of the noise.

$$Q = \begin{bmatrix} \boldsymbol{q_a} & \boldsymbol{0} & \boldsymbol{0} & \boldsymbol{0} \\ \boldsymbol{0} & \boldsymbol{q_g} & \boldsymbol{0} & \boldsymbol{0} \\ \boldsymbol{0} & \boldsymbol{0} & \boldsymbol{q_{ba}} & \boldsymbol{0} \\ \boldsymbol{0} & \boldsymbol{0} & \boldsymbol{0} & \boldsymbol{q_{bg}} \end{bmatrix}$$

$\boldsymbol{q_a}$=var($\boldsymbol{w_f}$) $\quad$ $\boldsymbol{q_{ba}}$= var($\boldsymbol{w_b}$) $= \sqrt{\boldsymbol{2\alpha\sigma^2}}^{\boldsymbol{2}}$

$\boldsymbol{q_g}$=var($\boldsymbol{w_w}$) $\quad$ $\boldsymbol{q_{bg}}$= var($\boldsymbol{w_d}$) $= \sqrt{\boldsymbol{2\beta\sigma^2}}^{\boldsymbol{2}}$

Global Positioning System (GPS)

It is a collection of 24 satellites divided into 6 different orbits around the earth and 4 satellites in each orbit. GPS is designed to be visible to at least four satellites in the sky anywhere on the planet at any given time.

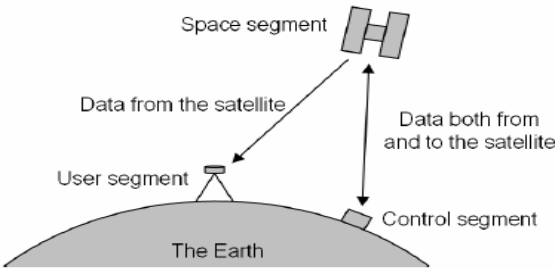

Figure 4-1- Components of the Global Positioning System[25]

Each satellite sends signals at a specific frequency concerning its position in the sky and the time when this information was sent. The GPS receiver, set in the transmitted signal bandwidth, can detect the time delay of the signal sent by satellite. Subsequently, it transfers this time delay to its distance from the satellite since the signal moves at the speed of light. In fact, a multi-channel receiver can receive a multi-satellite transmission signal simultaneously and calculate the signal latency of each satellite. Ideally, with an on-board processor, a receiver can calculate its position on the device using information received from three satellites. On the other hand, because the clock pulse on the board is almost always different from the GPS clock timing, there will always be a time bias to consider. Therefore, the measured distance between the receiver and the satellite is called pseudo-distance, and at least four satellites are needed to identify the position [16].
It is worth noting that all the raw GPS positioning information will be earth-centered, earth-fixed (ECEF) three-dimensional cartesian devices.
Now, if the position of the ith satellite is equal to (xi, yi, zi) in relation to the ECEF device, and also the position of the receiver in this device is equal to (x, y, z) and Δ is the bias of the receiver clock signal, and c is the speed of light and distance capture is ρi relative to this satellite, then these variables are related as follows:

$$(x - x_i)^2 + (y - y_i)^2 + (z - z_i)^2 = (\rho_i - c\Delta)^2$$

$$i = 1.2.3.4$$

The above equation can be summarized as follows:

$$\rho_i = r_i + b$$

$$\boldsymbol{b} = \boldsymbol{c}\Delta$$

$$\boldsymbol{r_i} = \sqrt{(\boldsymbol{x} - \boldsymbol{x_i})^2 + (\boldsymbol{y} - \boldsymbol{y_i})^2 + (\boldsymbol{z} - \boldsymbol{z_i})^2}$$

B is the bias of the clock signal normalized by the speed of light and ri is the actual distance of the receiver from the satellite.

Integrated Structures of INS and GPS

As stated, the advantages of each system can be used to cover the flaw of the other and increase the accuracy of the navigation by combining the output data of INS and GPS navigation systems.
As a result, even in the worst navigation conditions, the Integrated navigation system will be more accurate than the inertial navigation system.
Therefore, the integrated navigation system has a limited error during the navigation time, along with reducing the amount of error caused by the modeling of the gravitational acceleration and the calculations made in the navigation computer. Also, this system has the characteristic of inertial navigation systems, like real-time and continuous output with high-speed data acquisition.
The available structures to combine the inertial navigation system with GPS includes four general categories:

- Uncoupled system (simple combining)
- Loosely coupled (cascade)
- Tightly coupled
- Ultra-tightly coupled (deeply integrated)

In uncoupled systems, each system does its navigation calculations separately, and a simple integrations algorithm works on their output. In other words, the position is set by the GPS and is considered as the input for the inertial navigation system. This method is the easiest, cheapest, and fastest way to combine the said systems and requires a navigation computer with low memory. No feedback data exists in this method,

Furthermore, each system's malfunction does not affect the other one. This method has the lowest optimization accuracy compared to other coupling methods.

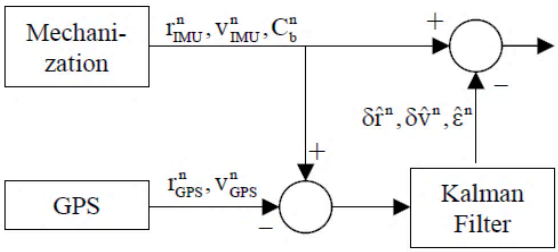

Figure 5-1- Uncoupled system structure

In the coupling structure, each system also does its calculations separately. However, there is feedback information in each of them from the results of the integration algorithm. This information is used to track the satellite's signal by the GPS receiver and correct the natural error of each system. The system is divided into two loosely or tightly coupled, based on whether or not the output of the Kalman filter is given to the GPS receiver as feedback.
In the loosely coupled method, the measurings of the GPS receiver are processed separately and then entered the Kalman filter with the Inertial navigation data. Kalman filter estimates the inertial navigation system's error level by processing the measurements of both systems. Then, it calculates the difference between these values from the output of inertial navigation and replaces the new values as the output of the inertial navigation.
In other words, the Kalman filter calculates the inertial navigation system error values.

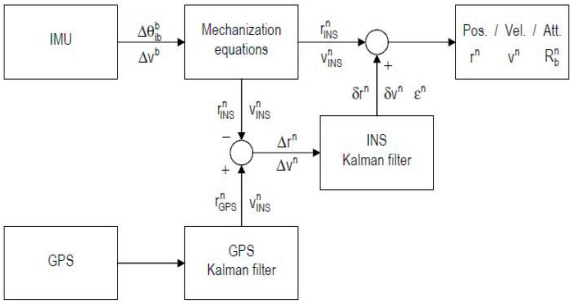

Figure 5-2- loosely coupled integration structure

The inertial navigation system is used as a reference path in the tightly coupled method. Therefore, the distance between the receiver and satellite is calculated based on the output of the inertial navigation system, and the difference of these values is used as the measures of the integration filter.
The ultra-tightly coupled method is a developing method. This method's principles are almost like the tightly coupled method. It is claimed that this method is more accurate than the previous methods. However, it has heavy loads of calculations [5-9] and [17-19].

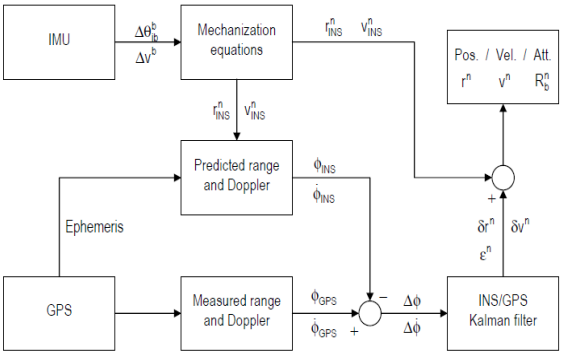

Figure 5-3- Tightly coupled integration structure

Nine parameters are needed to describe the inertial navigation system's behavior, including three position parameters, three velocity parameters, and three attitude parameters. In other words, it is necessary to have nine parameters to simulate the error system of inertial navigation in the loosely coupled method. However, in addition to these parameters, the describing equations of the receiver clock bias and accelerometer and gyroscope biases are also needed in the tightly coupled method. Therefore, the tightly coupled equation system includes more parameters, increasing the calculation complexity while having slightly better accuracy than the loosely coupled method. The difference between the tightly and loosely coupled methods is in the output data of the GPS receiver. The output data of the GPS receiver in the tightly coupled method includes pseudo-distance and its change rate. Also, the error of the GPS attitude is estimated by a Kalman filter. Nevertheless, in the loosely coupled system, the output data of the GPS receiver include position or speed, which are obtained from raw information (pseudo-distances)[28-30].

GPS measurement modeling (Posteriori estimation)

The raw measurements of the GPS receiver are in two forms: pseudo-distance and pseudo-velocity (pseudo-distance rate). As described in the GPS receiver model, pseudo-distance refers to the GPS receiver's measurement of the distance between the GPS satellite and the receiver, which is subject to error due to various factors. Pseudo-distance refers to measuring the relative velocity of the receiver and GPS satellite along the vision of the receiver from the GPS satellite, which is done by the Doppler method. This measurement is also affected by error factors.

In updating the posterior estimation (corrected) of the Kalman filter, which is done using the measurements of the GPS receiver, the difference between the measurements of the GPS receiver and the prediction of the estimate system from pseudo-distance and pseudo-velocity are entered into the coupling system as the measurement of the Kalman filter [5-9 and 16 and 24].

The prediction of the pseudo-distance ρ_{est}^{j} and pseudo-velocity ρ_{est}^{j}estimation system for each satellite are as follows:

$$\rho_{est}^{j} = \left| r_{GPS}^{j} - r \right|$$

$$\dot{\rho}_{est}^{j} = (v_{GPS}^{j} - v) \times \frac{(r_{GPS}^{j} - r)}{\left| r_{GPS}^{j} - r \right|}$$

In the above equation, $r_{GPS}^{j}$and v_{GPS}^{j} are the position and speed of the satellite j that the receiver is able to receive its signal.

r and v are also position and velocity estimates based on inertial navigation output data. Thus, the difference between GPS measurement and estimation, which is the same as observation vector, will be as follows:

$$Z_{measurment}^{j} = \begin{bmatrix} \rho^{j} \\ \dot{\rho}^{j} \end{bmatrix} - \begin{bmatrix} \rho_{est}^{j} \\ \dot{\rho}_{est}^{j} \end{bmatrix}$$

$$\boldsymbol{Z^{j} = H^{j} X} = \begin{bmatrix} \boldsymbol{U_i^j} & \mathbf{0_{1*3}} & \mathbf{0_{1*3}} & \mathbf{0_{1*3}} & \mathbf{0_{1*3}} \\ \mathbf{0_{1*3}} & \boldsymbol{U_i^j} & \mathbf{0_{1*3}} & \mathbf{0_{1*3}} & \mathbf{0_{1*3}} \end{bmatrix} \begin{bmatrix} \boldsymbol{r} \\ \boldsymbol{v} \\ \boldsymbol{\varepsilon} \\ \boldsymbol{\delta b} \\ \boldsymbol{\delta d} \end{bmatrix}$$

Where U_i^j is the normalized vector in the earth-centered, earth-fixed with unit length received from the j-th satellite by the GPS receiver and is obtained from the following equation:

$$U_i^j = \frac{(r_{GPS}^{j} - r)}{\left| r_{GPS}^{j} - r \right|}$$

Estimating and correcting navigation error using Kalman filter

The equations used in the Kalman filter are of two categories: the prediction of the state over time and the state of correction equations based on measurement. Thus, the state prediction equations must be calculated in each navigation calculation step to obtain the previous state estimate. Therefore, first, the equations of the continuous state space must be transformed into a discrete form: [20-23]

$$\emptyset_k = (I_{15*15} + F\Delta t)$$

$$x_{k+1} = \emptyset_k x_k + w_{dk}$$

Where, w_{dk} is the discrete process noise, which is obtained in terms of continuous time process noise as follows:

$$w_d[k] = N(0. Q_d[k])$$

$$Q_k = G(t_k) Q(t_k) G^T(t_k) \Delta t$$

The following equations show the previous state estimation and its covariance error with respect to the posterior state estimation and its covariance in the previous step [25-27]:

$$\hat{x}_{k+1}^{-} = \emptyset_{k+1}\hat{x}_{k}^{+}$$

$$p_{k+1}^{-} = \emptyset_{k+1}p_{k}^{+}\emptyset^{T}{}_{k+1} + Q_k$$

It should be noted that since the sampling rate in GPS (10 Hz) is much lower than inertial navigation (100 Hz), the prediction and estimation of the previous state are calculated based on the values of the previous step predictions until the observation is updated by GPS information to receive new information.

With each measurement of the information received from the satellites, the following matrix H is formed, and the observation matrix will be obtained based on it:

$$H = [H^{j} \quad H^{j+1} \ldots \quad H^{k}]^{T}$$
$$Z = [Z^{j} \quad Z^{j+1} \ldots \quad Z^{k}]^{T}$$

Now, by calculating kalman gain and updating the state estimation, the latter state estimation is obtained:

$$\hat{x}_{k+1}^{+} = \hat{x}_{k+1}^{-} + K_{k+1}(Z_{measurment} - H\hat{x}_{k+1}^{-})$$

$$P_{k+1}^{+} = (I - K_{k+1}H)P_{k+1}^{-}$$

$$K_{k+1} = P_{k+1}^{-}H^{T}(HP_{k+1}^{-}H^{T} + R)^{-1}$$

Where, R is the GPS measurement noise matrix and can be calculated from the GPS catalog using GPS measurement error sources.

$$R = \begin{bmatrix} \sigma_{r_{GPS}}^{2} & 0_{3*3} \\ 0_{3*3} & \sigma_{v_{GPS}}^{2} \end{bmatrix}$$

simulation results

The following values were considered for the simulations according to the relationships and explanations of Section 3 and Section 5:

The following values are obtained for the Markov noise parameters of accelerometers and gyroscopes:

$$\sqrt{q_a} = 300e-6 \ {}^{g}/_{\sqrt{Hz}}$$

$$\sqrt{q_g} = 220 \ {}^{(deg/h)}/_{\sqrt{Hz}}$$

$$\sigma_{ba} = 0.0077 \ \left({}^{m}/_{s^2}\right)$$

$$\tau_{ba} = 270 \ s \quad \Rightarrow \quad \sqrt{q_{ba}}$$

$$\sigma_{bg} = 192 \ \left({}^{deg}/_{h}\right)$$

$$\sqrt{q_{ba}} = 6.62e-4 \quad \Rightarrow \quad \sqrt{q_{ba}} = 0.004$$

Table 8-1: The initial condition of gps measurements for simulation

GPS standard deviation in length channel: σ_h	GPS standard deviation in width channel $\sigma_\emptyset$	GPS standard deviation in height channel σ_λ	GPS standard deviation for **VN**	GPS standard deviation for **VE**	GPS standard deviation for **VD**
$40m$	$3.14 \times 10^{-4} rad$	$3.14 \times 10^{-4} rad$	$9.16 \times 10^{-4} \ m$	$9.16 \times 10^{-4} \ m$	$12.64 \ m$

the position estimation in integrated navigation:

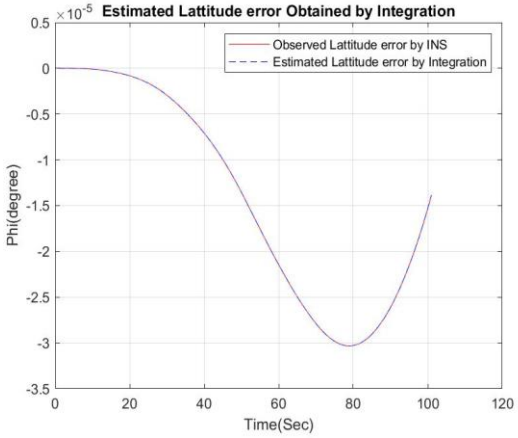

Figure 8-1: The latitude estimates

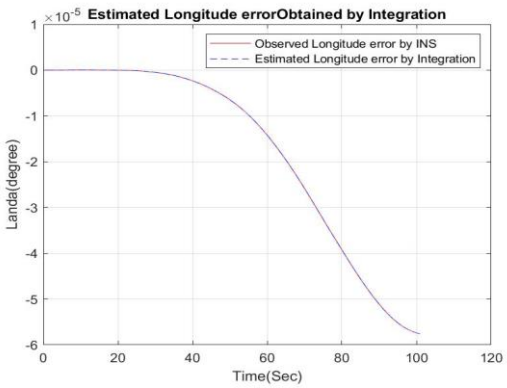

Figure 8-2: the longitude estimates

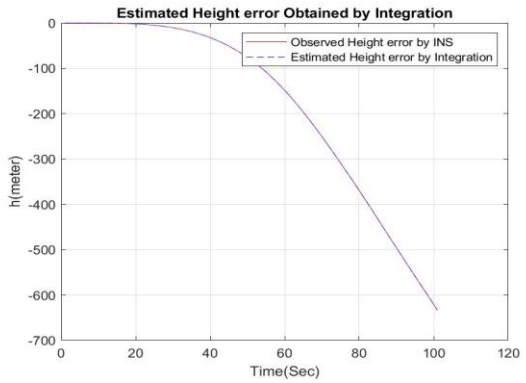

Figure 8-3: the height estimates

the velocity estimation in integrated navigation:

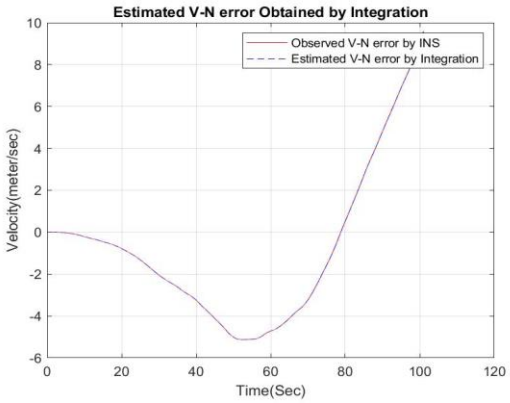

Figure 8-4: velocity estimate - north

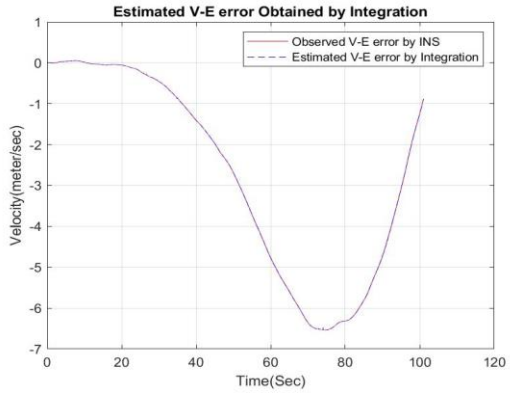

Figure 8-5: velocity estimate - east

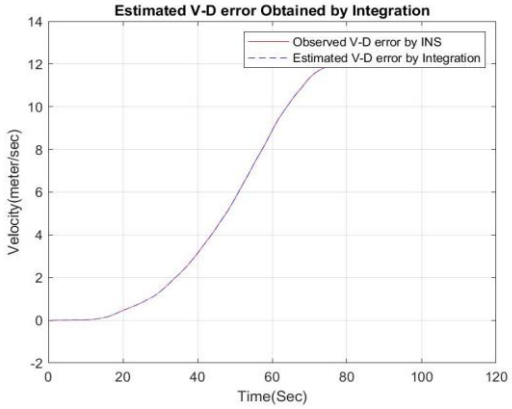

Figure 8-6: velocity estimate - south

the attitude estimation in integrated navigation:

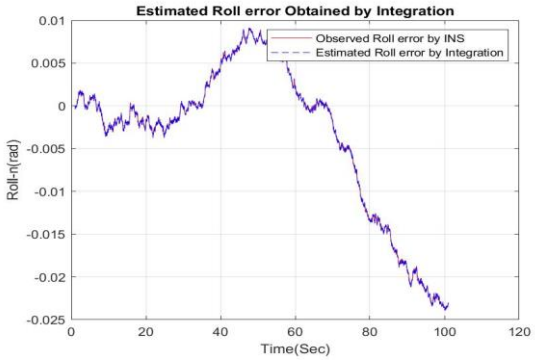

Figure 8-7: the roll estimates

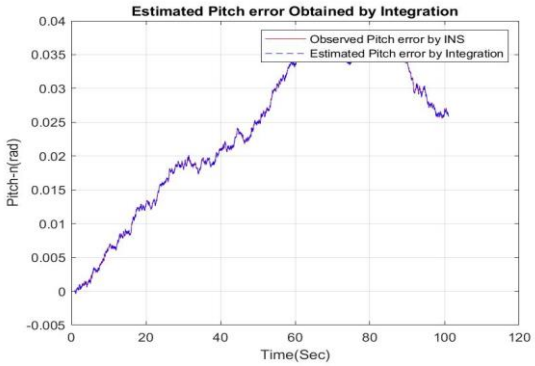

Figure 8-8: the pitch estimates

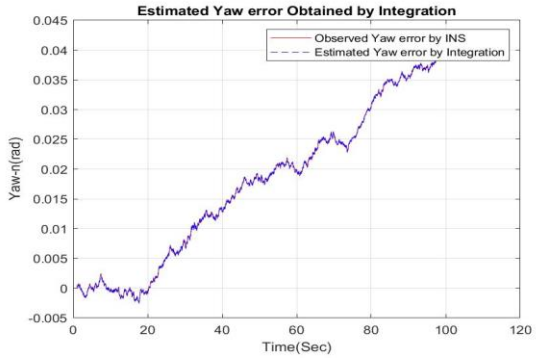

Figure 8-9: the yaw estimates

the accelerometer estimation in integrated navigation:

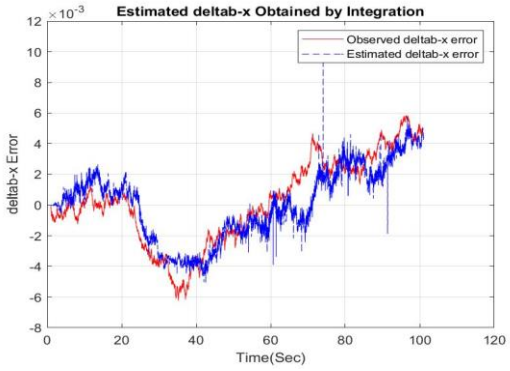

Figure 8-10: the accelerometer estimation along the x axis:

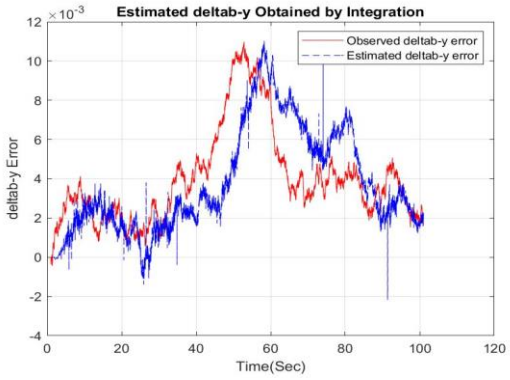

Figure 8-11: the accelerometer estimation along the y axis:

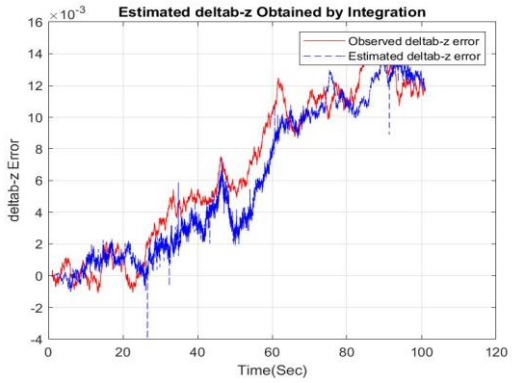

Figure 8-12: the accelerometer estimation along the z axis:

the gyroscope drift estimates in integrated navigation:

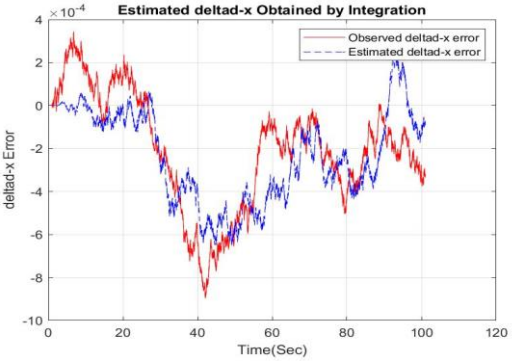

Figure 8-13: the gyroscope drift estimates along the axis

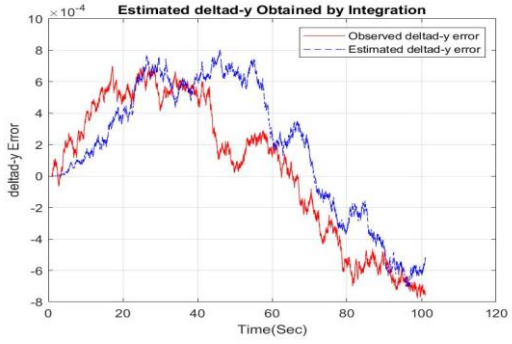

Figure 8-14: the gyroscope drift estimates along the y axis

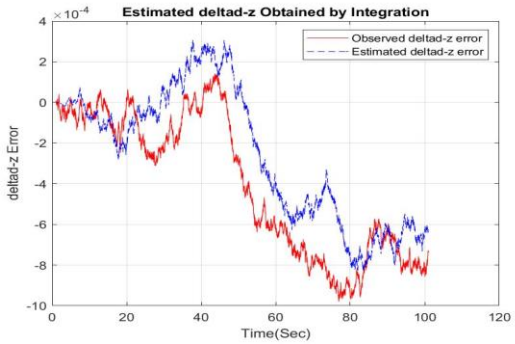

Figure 8-15: the gyroscope drift estimates along the z axis

Validation of position estimates:

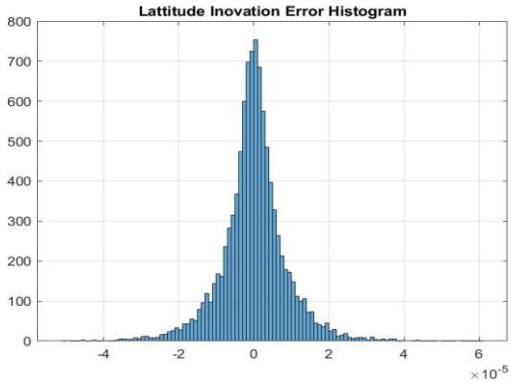

Figure 8-16: Innovation Signal Histogram Latitude Estimation Error

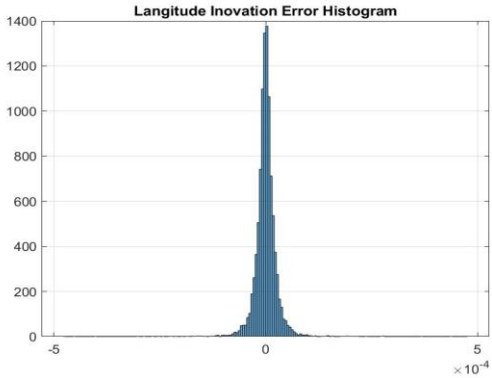

Figure 8-17: Innovation Signal Histogram longitude Estimation Error

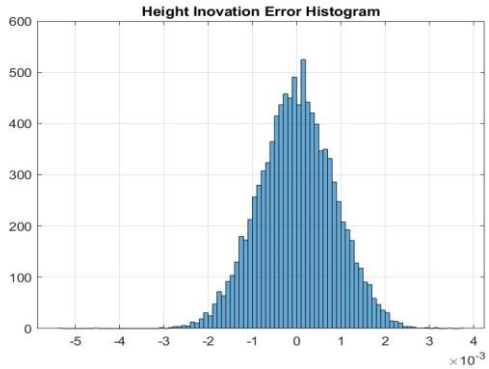

Figure 8-18: Innovation Signal Histogram Height Estimation Error

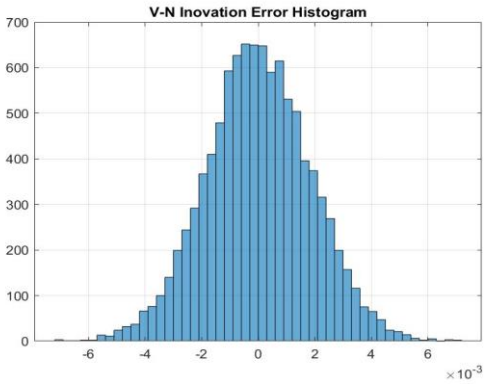

Figure 8-19: Innovation Signal Histogram velocity Estimation Error - north

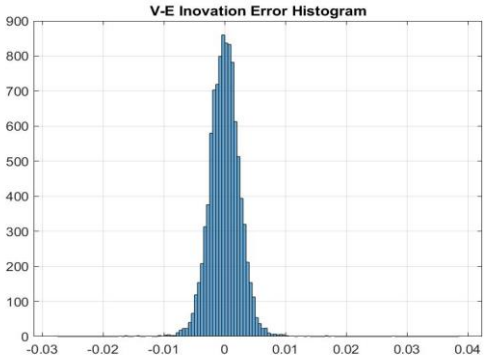

Figure 8-20: Innovation Signal Histogram velocity Estimation Error -east

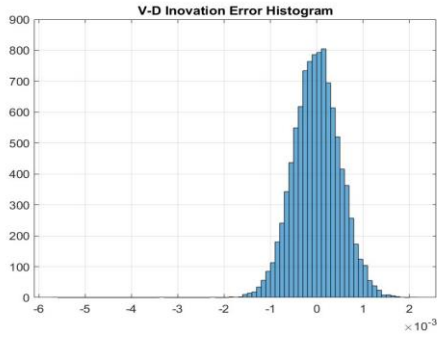

Figure 8-21: Innovation Signal Histogram velocity Estimation Error - south

Simulation Results Summary:

Table 8-21: simulation results summary
Results Analysis

Fusion Feedback														
RMS of State Estimate Error														
Lat.	Long.	height	V-N	V-E	V-D	Roll	Pitch	Yaw	bx-drift	by-drift	bz-drift	dx-drift	dy-drift	dz-drift
1.8e-05	2.6e-5	263.4	3.72	3.68	8.10	0.0096	0.0260	0.0218	0.0023	0.0046	0.0076	0.0001	0.0004	0.0004
Fusion Feedback Outage (Short Time)														
RMS of State Estimate Error														
Lat.	Long.	height	V-N	V-E	V-D	Roll	Pitch	Yaw	bx-drift	by-drift	bz-drift	dx-drift	dy-drift	dz-drift
1.35e-7	1.73e-7	2.9602	0.163	0.191	0.197	0.0037	0.0031	0.0031	0.0024	0.007	0.0015	0.0003	0.0002	0.0002
Fusion Feedback Outage (Long Time)														
RMS of State Estimate Error														
Lat.	Long.	height	V-N	V-E	V-D	Roll	Pitch	Yaw	bx-drift	by-drift	bz-drift	dx-drift	dy-drift	dz-drift
1.20e-7	1.45e-7	3.40	0.180	0.178	0.260	0.0059	0.0039	0.0045	0.0031	0.003	0.0022	0.0002	0.0002	0.0002

As it is clear from the first row of the above table, all 9 state estimations were well estimated, including the position, velocity, and attitude of the flying object, along with the biases of the accelerometers and the drifts of the gyroscopes. However, the main advantage of this article in estimating the above 15 states is the outage of the GPS signal for a short or long period. Such a procedure in most integrated estimation algorithms will lead to divergence of the estimations or less accurate results. The main reason is that the GPS information is considered the reference signals of the estimation observations in the integrated estimation. Therefore, if they are not available, we will not have a correct estimation. However, in this article, even though the GPS signal was not available at times, the estimation of the states did not deteriorate and had higher accuracy than the first estimation (rows 1), which can be seen in rows 2 and 3 of the above table. This result was obtained with the help of the estimation algorithm proposed in this article.

This paper attempted to reduce the inertial navigation error, which increases over time and improves the navigation accuracy by using a fully integrated inertial navigation system and GPS model. As can be concluded from the simulation results in Section 8, the position, velocity, and attitude of the flying object have been estimated with good accuracy in 3 scenarios. First, the Gps and INS were integrated without a GPS outage signal. In the second scenario, the GPS signal was outage for 4 seconds, while the integration method helped improve the estimation accuracy. At last, in the third scenario, the outage of the GPS signal was prolonged. However, good accuracy was also obtained in this scenario.

Despite the GPS outage signal, all of these improvements were achieved due to the tightly coupled integration suggested in this paper.

These estimates were validated by displaying the innovation signal of the estimation error. Since a good estimate has an Innovation signal with white noise characteristics, the histogram

of this signal for speed and position showed that the estimation is acceptable.

Also, the bias estimation of accelerometers and drift of gyroscopes were done with acceptable accuracy but not as accurate as the estimation of the first 9 parameters since these six parameters were unobservable. Of course, the validation of these estimates was done by another method, plotting the error variance diagram. Therefore, it was observed that the variance of the estimation error tends to the error covariance matrix, and their difference tends to zero, which indicates a good estimate of these 6 parameters.

Finally, the RMS estimation error and self-estimation of 15 navigation parameters are summarized in tables 8-2.

Of course, it is important to note that the error model was not considered for GPS, and its five errors were omitted. Also, other errors involved in the deviation of accelerometers and gyroscopes, such as scale errors, were omitted. If these errors were considered, this model would be a 27-state model. Nevertheless, they were omitted due to the prevention of computational complications and their smallness compared to other errors.

Reference

[1] Chiang, K. W., H. Hou, X. Niu and N. El-Sheimy, "Improving the Positioning Accuracy of DGPS/MEMS IMU Integrated Systems Utilizing Cascade De-noising Algorithm", in Proceedings of ION GPS, pp. 809-818, U. S. Institute of Navigation, 2004.

[2] Cao, F.X., Yang, D.K., Xu, A.G., \ Low Cost SINS/GPS Integration for Land Vehicle Navigation," IEEE International Conference on Intelligent Transport Systems, Singapore, 2002.

[3] Panzieri, S., Pascucci, F., Ulivi, G., "An Outdoor navigation system using GPS and Inertial Platform," IEEE ASME Transactions on Mechatronics, Vol. 7, No.2, 2002.

[4] Noureldin, A., Karamat, T., & Georgy, J. "Faundamentals of Inertial Navigation, Satellite-based Positioning and their Integration", Springer-Verlag, 2012;

[5] Angrisano, A., Petovello, M.G. and Pugliano G., "GNSS/INS Integration in Vehicular Urban Navigation", Proceedings of GNSS10 (Portland, OR, 21-24 Sep), The Institute of Navigation,2010.

[6] El-Sheimy, N., "Inertial techniques and INS/DGPS Integration, ENGO 623-Course Notes", Department of Geomatics Engineering, University of Calgary, Canada, 2004.

[7] El-Sheimy, N., K. P. Schwarz, M. Wei, and M. Lavigne , "VISAT: A Mobile City Survey System of High Accuracy", Proceedings of ION GPS , pp. 1307–1315. Institute Of Navigation,1995;

[8] Godha, S. , "Performance Evaluation of Low Cost MEMS-Based IMU Integrated With GPS for Land Vehicle Navigation Application", MSc Thesis, Department of Geomatics Engineering, University of Calgary, Canada, UCGE Report No. 20239. 164, 2006.

[9] Godha, S., Lachapelle, G. and Cannon, M.E. , "Integrated GPS/INS System for Pedestrian Navigation in a Signal Degraded Environment", Proceedings of ION GNSS06, 26-29 Sept., Fort Worth, Session A5, pp. 2151 – 2164, The Institute of Navigation, 2006.

[10]Nassar, S., "Improving the Inertial Navigation System (INS) Error Model for INS and INS/DGPS Applications", PhD Thesis, Department of Geomatics Engineering, University of Calgary, Canada, UCGE Report No. 20183, 2003.

[11] Chang L., Li K., Hu B.,"Huber's M-Estimation Based Process Uncertainty Robust Filter for Integrated INS/GPS", IEEE Sensor Journal, Vol. 15, No. 6, 2015.

[12] Gao, P., Li, K., Song, T., and Liu, Z., "An Accelerometers SizeEffect Self Calibration Method for Triaxis Rotational Inertial Navigation System", IEEE Transactions on Industrial Electronics, Vol. 65, No. 2, pp.1655-1664, 2018.

[13] Sun, Y., Yang, G., Cai, Q., and Wang, S., "An Online Calibration Method of SINS/Odometer Integrated Navigation System", 4th International Conference on Information Science and Control Engineering (ICISCE), 2017.

[14] Kim, Y., An, J., and Lee ,J., "Robust Navigational System for a Transporter Using GPS/INS Fusion", IEEE Transactions on Industrial Electronics, Vol.65, No.4, pp.3346-3354, 2018.

[15] Zhong M., Guo J., and Zhou D., "Adaptive in- Flight Alignment of INS/GPS Systems for Aerial Mapping", IEEE Transactions on Aerospace and Electronic Systems, Vol.99, pp.1-12, 2017.

[16] Li K., Zhao J., Wang X., Wang L.,"Federated Ultra-Tightly Coupled GPS/INS Integrated Navigation System Based on Vector Tracking for Severe Jamming Environment", IET Radar, Sonar and Navigation Journal, Vol. 10, No. 6, 2016.

[17] Chang, L., Hu, B., Li, A., Qin, F., "Strapdown Inertial Navigation System Alignment Based on Marginalised Unscented Kalman Filter", IET Journal ofScience, Measurement and Technology, Vol. 7. No. 2, pp. 128-138, 2013.

[18] Chang, L., Zha, F., and Qin, F., "Indirect Kalman Filtering Based Attitude Estimation for Low-Cost Attitude and Heading Reference Systems", IEEE/ASME Transactions on Mechatronics, Vol.22, No.4, pp.850-1858, 2017.

[19] Salamat, B., and Tonello, A.M., "Altitude and Attitude Tracking of a Quadrotor Helicopter UAV using a Novel Evolutionary Feedback Controller", International Conference on Smart Systems and Technologies (SST), 2017.

[20] Petovello, M., "Real-time Integration of a Tactical-Grade IMU and GPS for High-Accuracy Positioning and Navigation", PhD Thesis, Department of Geomatics Engineering, University of Calgary, Canada, UCGE Report No. 20173, 2003.

[21]Petovello, M., "Estimation for Navigation", ENGO 699.18 - Lecture Notes, Department of Geomatics Engineering, University of Calgary, Canada, 2009.

[22] Shin, E., "Accuracy Improvement of Low Cost INS/GPS for Land Application", MSc Thesis, Department of Geomatics Engineering, University of Calgary, Canada, UCGE Report No. 20156, 2001.

[23]Shin, E., "Estimation Techniques for Low-Cost Inertial Navigation", PhD Thesis, Department of Geomatics Engineering, University of Calgary, Canada, UCGE Report No. 20219, 2005.

[24] Klein I., Filin S. and Toledo T., "Pseudo-measurements as aiding to INS during GPS outages", Navigation 57(1), pp. 25-34, 2010.
[25] F M, K Saadeddin and M A Jarrah, "Constrained low-cost GPS/INS filter with encoder bias estimation for ground vehicles' applications [J]", Mechanical Systems and Signal Processing, vol. 58, pp. 285-297, 2015.
[26] H Zhao, Z Xiong, L Shi et al., "A robust filtering algorithm for integrated navigation system of aerospace vehicle in launch inertial coordinate[J]", Aerospace Science and Technology, vol. 58, pp. 629-640, 2016.
[27] G Chang and M. Liu, "Hybrid Kalman and unscented Kalman filters for INS/GPS integrated system considering constant lever arm effect[J]", Journal of Central South University, vol. 22, no. 2, pp. 575-583, 2015.
[28] S Häfner and R Thomä, "Extended Kalman Filtering and Maximum-Likelihood Estimation for Point Target Localisation[C]", *2020* German Microwave Conference. IEEE, pp. 116-119, 2020.
[29] R. Wang, X. Hou, F. Liu and Y. Yu, "GPS/INS Integrated Navigation for Quadrotor UAV Considering Lever Arm," 2020 35th Youth Academic Annual Conference of Chinese Association of Automation (YAC), 2020, pp. 132-136.
[30] C. Jiayao, Z. Dalong, H. Gangtao and L. Zhiyuan, "A Method for Lever Arm Estimation in INS/GPS Integration Using Direct Unscented Kalman Filter," 2020 IEEE 6th International Conference on Computer and Communications (ICCC), 2020, pp. 985-990.